# Experimental and Computational Studies of Nuclear Substituted 1,1′-Dimethyl-2,2′-Bipyridinium Tetrafluoroborates

**Dong Zhang,[†] João P. Telo,[‡] Chen Liao,[†] Sean E. Hightower,[†] and Edward L. Clennan*,[†]**

*Department of Chemistry, University of Wyoming, Laramie, Wyoming 82071, and Instituto Superior Técnico, Química Orgânica, Av. Rovisco Pais, P-1049-001 Lisboa, Portugal*

*Received: June 4, 2007; In Final Form: September 6, 2007*

The synthesis and spectral properties of a new 2,2′-bipyridinium ion, 1,1′-dimethyl-4,4′-(dimethylamino)-2,2′-bipyridinium bis(tetrafluoroborate) are reported. Rotation of the dimethylamino group is slow at room temperature on the 400 MHz $^1$H and 100 MHz $^{13}$C NMR time scales. Complete line shape fit of the dynamically broadened NMR spectra was used to determine the activation barriers for this process. The first complete set of UV−vis spectra for a 2,2′-bipyridinium dication and its one- and two-electron reduced products was reported. TD−DFT calculations were used to help assign the origin of the long wavelength absorptions in these species. The effect of substituents on the energies and conformational potential energy surfaces of all three species were also examined using the B3LYP/6-31G(d) computational method.

## Introduction

1,1′-Dimethylbipyridinium ions (e.g., $\mathbf{1}^{2+}$ and $\mathbf{2}^{2+}$) have been known since 1882.[1] The 4, 4′ isomer, $\mathbf{1}^{2+}$, was introduced as an oxidation−reduction indicator by Michaelis in 1932 and referred to as methyl viologen.[2] Intense interest in these compounds did not develop, however, until the discovery in the mid-1950s that several derivatives functioned as potent herbicides.[3] More recently, they have found widespread use as components of electrochromic display devices and of supramolecular structures,[4] as acceptors in molecular assemblies designed to store solar energy via long-lived charge separation,[5] and as relays in electron-transfer events.[6]

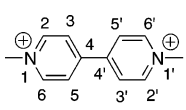

$\mathbf{1}^{2+}$

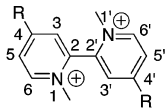

$\mathbf{2}^{2+}$ R = H
$\mathbf{3}^{2+}$ R = $NMe_2$
$\mathbf{4}^{2+}$ R = Cl
$\mathbf{5}^{2+}$ R = OMe
$\mathbf{6}^{2+}$ R = $CO_2Me$

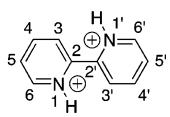

$\mathbf{7}^{2+}$

These important materials are invariably made by alkylation of a bipyridine precursor. The wide spectrum of alkylating agents that successfully react has allowed incorporation of both 4,4′- and 2,2′-bipyridinium ions in a wide variety of novel molecular scaffolds. However, with the exception of our earlier report,[7] derivatives with heteroatom substitutents on the carbon framework of the bipyridinium ion core of these materials, are extremely rare. In this previous study[7] we examined both the electrochemical and optical properties of a series of 2,2′-bipyridinium ions in anticipation that they would function as electron-transfer sensitizers in charge shift reactions with neutral substrates to give a repulsive cation-radical/cation-radical pair whose rapid separation would compete with back electron transfer. We also reported the first nanosecond transient absorption spectra of bypyridinium ions that have been attributed to the triplet excited state. Consistent with this observation we also demonstrate the bipyridinium sensitized formation of singlet oxygen ($^1\Delta_g$) and its trapping by 2,3-dimethyl-2-butene to give an allylic hydroperoxide. We report here the synthesis and characterization of the new heteroatom substituted 2,2′-bipyridinium derivative 1, 1′-dimethyl-4,4′-(dimethylamino)-2,2′-bipyridinium tetrafluoroborate, $\mathbf{3}^{2+}$. We also report new spectroscopic data for $\mathbf{6}^{2+}$, its radical cation, and neutral analogue, and a DFT study of the conformational potential energy surface of bipyridinium ions $\mathbf{1}^{2+}$, $\mathbf{2}^{2+}$, $\mathbf{3}^{2+}$, $\mathbf{4}^{2+}$, $\mathbf{5}^{2+}$, $\mathbf{6}^{2+}$, and $\mathbf{7}^{2+}$ and both of their redox partners (Figure 1).

## Results and Discussion

**1,1′-Dimethyl-4,4′-(dimethylamino)-2,2′-bipyridinium Tetrafluoroborate, $\mathbf{3}^{2+}$.** The synthetic route used to make $\mathbf{3}^{2+}$ is depicted in Figure 2. 2,2′-Bipyridine *N*,*N*′-dioxide, **8**, was formed in 94% yield by treatment of 2,2′-bipyridine with 30% hydrogen peroxide in glacial acetic acid at 70−80 °C.[8] This off white material was then converted in 52% yield to the yellow powder 4,4′-dinitro-2,2′-bipyridine *N*,*N*′-dioxide, **9**, by treatment with a mixture of fuming sulfuric and nitric acids.[9] The nitro groups in **9** were replaced with chlorine in 80% yield using acetyl chloride in glacial acetic acid to give 4,4′-dichloro-2,2′-bipyridine *N*,*N*′-dioxide, **10**.[10] The chlorines in **10** are subsequently readily exchanged with dimethylamino groups by refluxing in DMF.[10] This exchange reaction does not occur in the bipyridine but requires the activation afforded by the *N*-oxide groups. The oxygens can be removed from the crude brown paste containing **11** by treatment with $PCl_3$ in a low but acceptable yield (19%) to given 4,4′-(dimethylamino)-2,2′-bipyridine, **12**.[10] Treatment of **12** with 2 equiv of trimethyloxonium tetrafluoroborate[11] generated, after three recrystallizations from acetonitrile/diethyl ether a 75% yield of analytically pure beige bipyridinium salt $\mathbf{3}^{2+}$.

The $^{13}$C and $^1$H NMRs of $\mathbf{3}^{2+}$ both exhibited signals for three magnetically distinct methyl groups. In the $^{13}$C NMR spectrum ($CD_3CN$) two peaks for the $-N(CH_3)_2$ groups were observed at 41.10 and 41.19 ppm and a peak for the pyridinium $N-CH_3$

[†] University of Wyoming.
[‡] Instituto Superior Técnico.

10.1021/jp074323u CCC: $37.00 
Published on Web 12/20/2007

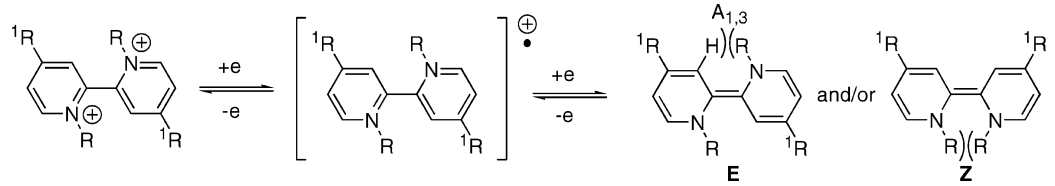


**Figure 1.**

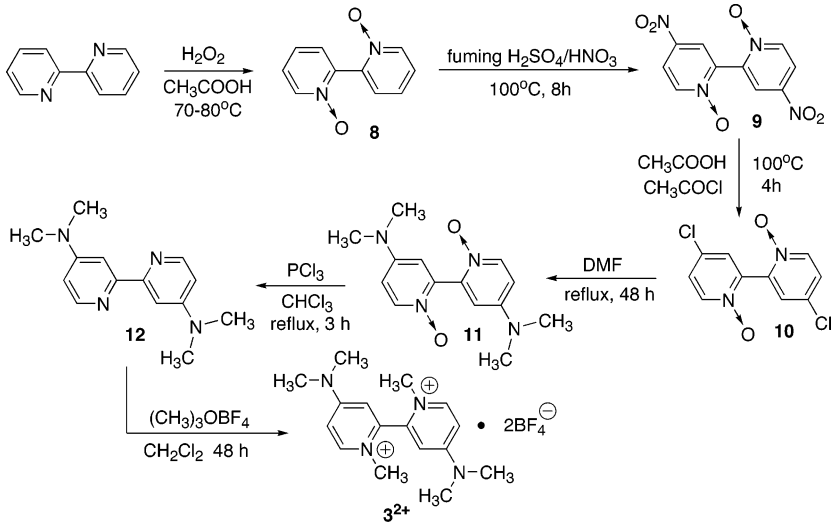


**Figure 2.**

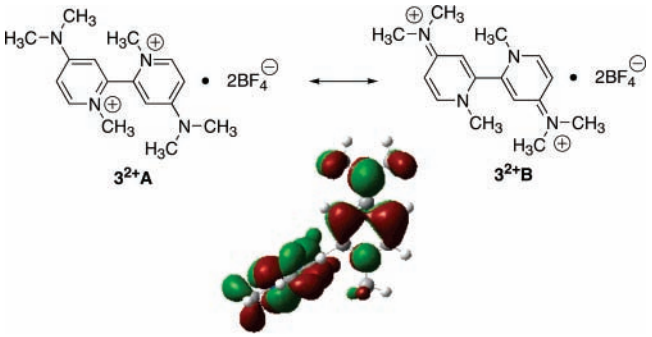


**Figure 3.**

at 43.76 ppm. In the $^1$H NMR spectrum two six hydrogen singlets for the -N(CH$_3$)$_2$ groups were observed at 3.19 and 3.25 ppm and a singlet for the pyridinium N−CH$_3$ at 4.60 ppm. In D$_2$O above 40 °C at 400 MHz the two −N(CH$_3$)$_2$ singlets (3.20 and 3.26 ppm) broaden and finally coalesce at approximately 68 °C to a broad singlet (see Supporting Information).

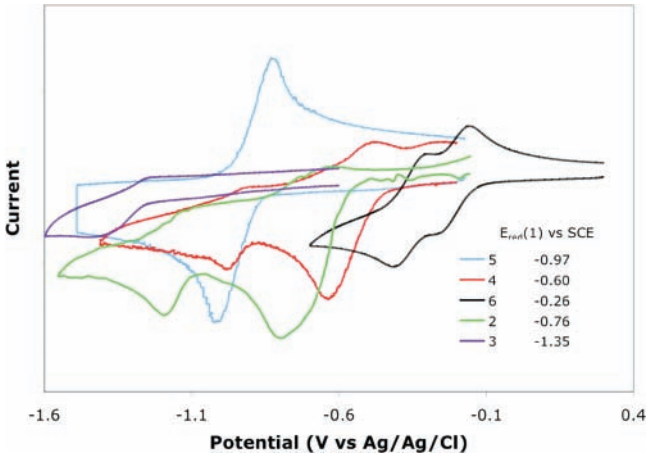


**Figure 4.** Cyclic voltammograms for bipyridinium ions **2**−**6**.

These results are consistent with a significant contribution of resonance form **3**$^{2+}$**B** to the ground state electronic description of the bipyridinium dication **3** leading to restricted rotation at room temperature around the (CH$_3$)$_2$N−pyridinium bond (Figure 3). A contribution of resonance form **3**$^{2+}$**B** is also consistent with the B3LYP/6-31G(d) HOMO (Figure 3), which exhibits significant $\pi$-electron density between the −N(CH$_3$)$_2$ group and the ring carbon. A complete line shape fit[12] to the two site exchange broaden spectra give $\Delta H^{\ddagger} = 13.23$ kcal/mol, $\Delta S^{\ddagger} = -11.9$ cal/(mol·K), and $\Delta G^{\ddagger}(298.16\text{K}) = 16.9$ kcal/mol. The Gibbs free energy of activation at 355 K is nearly identical to that reported (17.6 kcal/mol) for rotation about the nitrogen ring carbon bond in 1-methyl-4-(methylamino)pyridinium perchlorate[13] at the same temperature, suggesting that the pyridinium ion substituent plays little if any steric or electronic role in dictating the magnitude of the rotation barrier. The lack of a steric effect is perhaps not surprising given the nearly perpendicular arrangement (vide infra) of the two pyridinium rings in the dication.

The cyclic voltammetic behavior of **3**$^{2+}$ is compared to that of **2**$^{2+}$, **4**$^{2+}$, **5**$^{2+}$, and **6**$^{2+}$ in Figure 4.[7] As anticipated, on the basis of the strong electron donating ability of the dimethylamino group, 2,2′-bipyridinium ion **3**$^{2+}$ proved the most difficult to reduce (Figure 1). In fact, a plot of the reduction potentials versus the appropriate Hammett substituent constant ($\sigma_p$) exhibits a straight line ($\rho = 0.98$; $R^2 = 0.9845$; see Supporting Information) with a slope indicative of substantial electronic interaction of the substituent with the bipyridinium core. A wide spectrum of electrochemical behavior is observed in these substitutional isomers. Only the bis(carbomethoxy)-substituted 2,2′-bipyridinium ion **6**$^{2+}$ exhibited two reversible electrochemi-

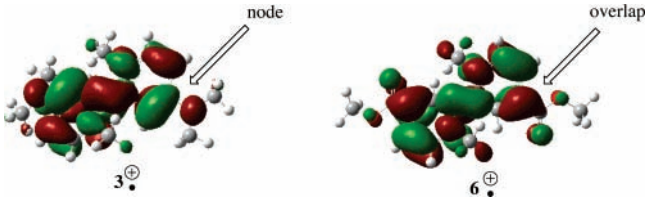


**Figure 5.** B3LYP/6-31G(d) SOMO's of the radical cations of **3** and **6**.

cal CV peaks for the two redox couples depicted in Figure 1. We attribute the apparent instability of all the radical cations with the exception of $\mathbf{6}^{+\bullet}$ to the inability to attain the electronically preferred planar radical cation geometry (vide infra). The bis(carbomethoxy) substituent, however, provides resonance delocalization of the $\mathbf{6}^{+\bullet}$ SOMO that is not available with other substitutents. This resonance stabilization is clearly evident in Figure 5 that shows significant overlap between the carbomethoxy group and the ring carbon in the B3LYP/6-31G(d) SOMO of $\mathbf{6}^{+\bullet}$ but a node between the ring carbon and the dimethylamino group in $\mathbf{3}^{+\cdot}$.

The unique character of the carbomethoxy group has allowed the first measurement of the UV−vis spectra of all three redox partners in a 1,1′-dimethyl-2,2′-bipyridium salt, as shown in Figure 6. A long wavelength electronic absorption maximum was observed at 296 nm in $\mathbf{6}^{2+}$ and at 645 nm in **6**. In $\mathbf{6}^{+\bullet}$, however, two long-wavelength electronic absorption maxima were observed at 1225 and 1435 nm. We tentatively assign one of these near-infrared absorption maxima to a charge-transfer (CT) band in the synclinal (*sc*) and the second to a CT band in the anticlinal (*ac*) conformation of $\mathbf{6}^{+\bullet}$ (vide infra). Time-dependent density functional theory (TD−DFT) calculations of the electronic spectra[14] for $\mathbf{6}^{2+}$ (266 nm; $f = 0.2191$) and **6** (613 nm; $f = 0.3241$) reasonably reproduced these absorption

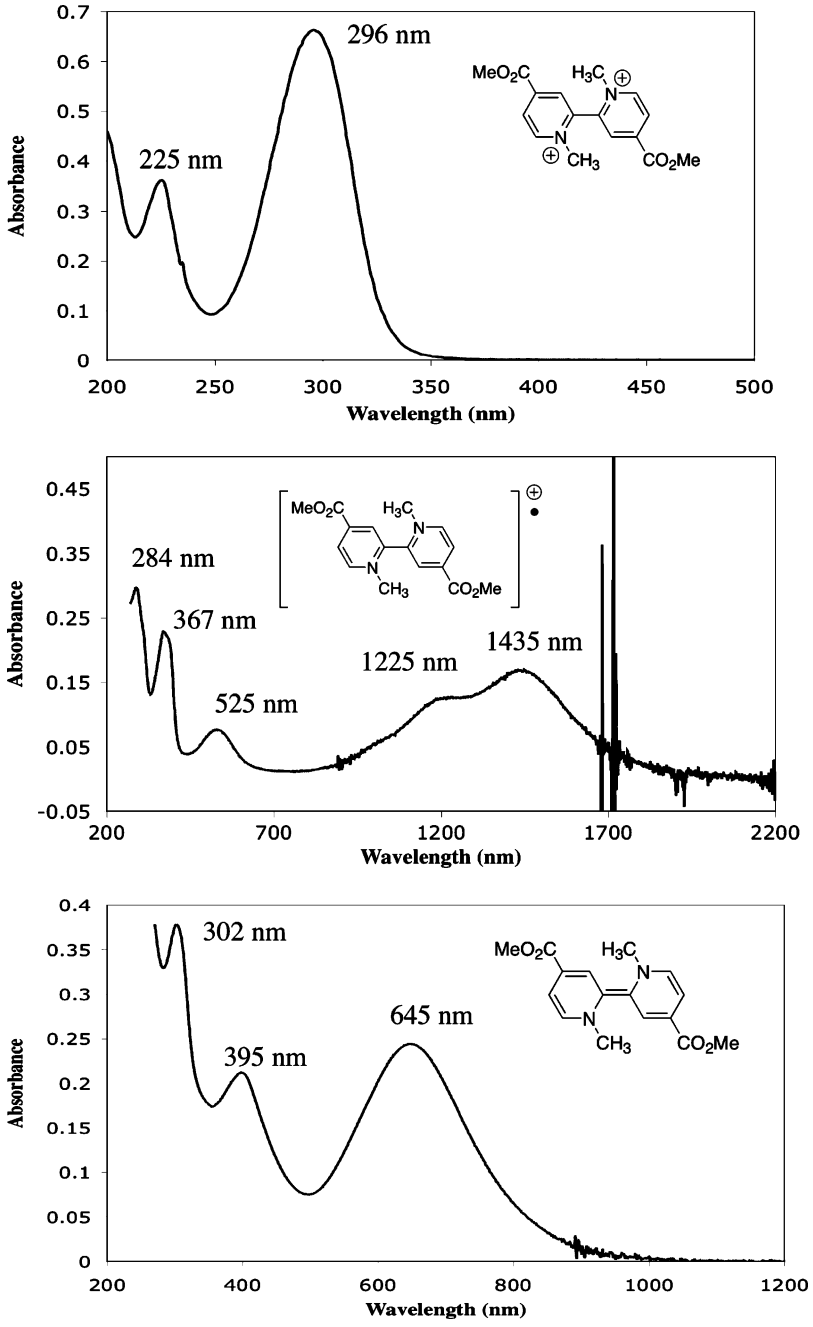


**Figure 6.** UV−vis spectra of $\mathbf{6}^{2+}$ (top), $\mathbf{6}^{+\bullet}$ (middle), and **6** in acetonitrile.

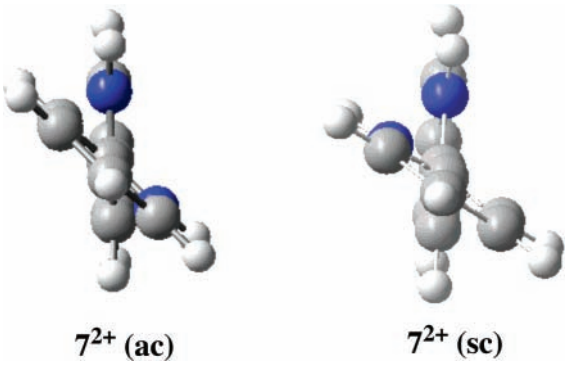


**Figure 7.**

**TABLE 1: Computed Structural Data for Bipyridinium Dications**

| compound | $d(C_2-C_{2'})$ (Å) | $\angle N_1C_2C_{2'}N_{1'}$ (deg) | $\Delta E_{relative}$ (kcal/mol) |
|---|---|---|---|
| $\mathbf{7}^{2+}$ | | | |
| ap: | | | 0 |
| B3LYP/6-31G(d) | 1.484 | 136.2 | |
| MP2/6-31G(d) | 1.478 | 127.4 | |
| MP2/6-31+G(d,p) | 1.479 | 125.0 | |
| sp: | | | 1.78 |
| B3LYP/6-31G(d) | 1.489 | 59.4 | |
| $\mathbf{2}^{2+}$ | 1.501 | 98.5 | |
| $\mathbf{3}^{2+}$ | 1.501 | 86.63 | |
| $\mathbf{4}^{2+}$ | 1.502 | 97.1 | |
| $\mathbf{5}^{2+}$ | | | |
| out-out[a] | 1.501 | 93.4 | 0 |
| in-out | 1.502 | 90.4 | 2.01 |
| in−in | 1.503 | 91.1 | 4.09 |
| $\mathbf{6}^{2+}$ | | | |
| in-in[b] | 1.499 | 109.8 | 0 |
| in-out | 1.500 | 103.7 | 1.58 |
| out−out | 1.500 | 99.4 | 3.02 |

[a] Alignment of in-plane O-methyl group; out-pointing away from the adjacent pyridinium ring and in-pointing toward adjacent pyridinium ring. [b] Alignment of in-plane carbonyl-oxygen; out-pointing away from the adjacent pyridinium ring and in-pointing toward adjacent pyridinium ring.

maxima. However, as anticipated by the well-established inability of TD−DFT to yield accurate excitation energies of charge-transfer excited states,[15] the calculated long wavelength absorption maximum of the most stable carbomethoxy rotomers (vide infra) of the *ac* (998 nm; $f = 0.1275$) and *sc* (1030 nm; $f = 0.1273$) conformations of $\mathbf{6}^{+\bullet}$ did not faithfully reproduce the experimental values. Long wavelength absorption was also detected in the spectrum of $\mathbf{5}^{+\bullet}$ (see Supporting Information) as a weak band without a clear maximum that extended out to nearly 1200 nm.

**Computational Studies.** Calculations were performed with the Gaussian 03 program[16] using the Becke/Stephens[17,18] three-parameter Lee−Yang−Parr correlation hybrid functional B3LYP in conjunction with the 6-31G(d) basis set. In the case of $\mathbf{7}^{2+}$ the performance of this model was compared to previously published STO-3G calculations[19] with partial geometry optimization and with MP2 calculations using the 6-31G(d) and 6-31+G(d,p) basis sets. Frequency calculations were used to verify location of energy minima. The absence of spin contamination was verified in each calculation by examination of $\langle S^2 \rangle$, which showed values acceptably close to 0 for all singlets and to 0.75 for all doublets.[20]

**Dication Redox Partners.** Two energy minima were located for 2,2′-bipyridinium dication, $\mathbf{7}^{2+}$, at all computational levels

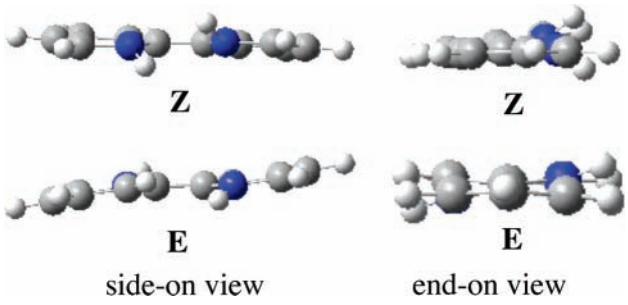


**Figure 8.**

**TABLE 2: Computed Structural Data for Bipyridinium Radical Cations[a]**

| compound | $\Delta E$ (kcal/mol) | $d(C_2C_{2'})$ (Å) | $\angle N_1C_2C_{2'}N_{1'}$ (deg) | $\angle CH_3N_1C_2C_{2'}$ (deg) |
|---|---|---|---|---|
| $\mathbf{2}^{+\bullet}$-*ac* | 0 | 1.445 | 140.82 | 17.24/17.00 |
| $\mathbf{2}^{+\bullet}$-*sc* | 1.56 | 1.446 | 44.43 | 20.85/28.37 |
| $\mathbf{3}^{+\bullet}$-*ac* | 0 | 1.441 | 142.20 | 19.63/20.37 |
| $\mathbf{3}^{+\bullet}$-*sc* | 0.25 | 1.441 | 40.85 | 29.57/28.44 |
| $\mathbf{4}^{+\bullet}$-*ac* | 0 | 1.445 | 141.35 | 17.23 |
| $\mathbf{4}^{+\bullet}$-*sc* | 1.63 | 1.447 | 45.18 | 22.61/27.72 |
| $\mathbf{5}^{+\bullet}$-*ac*-ii | 0 | 1.441 | 142.25 | 19.10 |
| $\mathbf{5}^{+\bullet}$-*ac*-io | 0.41 | 1.440 | 142.42 | 17.60[b]/19.12[c] |
| $\mathbf{5}^{+\bullet}$-*ac*-oo | 0.77 | 1.440 | 143.20 | 18.04 |
| $\mathbf{5}^{+\bullet}$-*sc*-ii | 0.75 | 1.442 | 42.32 | 27.34 |
| $\mathbf{5}^{+\bullet}$-*sc*-io | 1.31 | 1.442 | 42.42 | 28.41[b]/26.52[c] |
| $\mathbf{5}^{+\bullet}$-*sc*-oo | 2.19 | 1.443 | 42.50 | 27.50 |
| $\mathbf{6}^{+\bullet}$-*ac*-ii | 0 | 1.453 | 140.22 | 15.68 |
| $\mathbf{6}^{+}$.-*ac*-io | 1.03 | 1.453 | 139.35 | 16.49[d]/15.24[e] |
| $\mathbf{6}^{+\bullet}$-*ac*-oo | 2.01 | 1.454 | 138.25 | 15.78/15.75 |
| $\mathbf{6}^{+\bullet}$-*sc*-ii | 2.80 | 1.455 | 47.54 | 19.44/26.63 |
| $\mathbf{6}^{+\bullet}$-*sc*-io | 3.13 | 1.455 | 47.27 | 27.18[d]/19.06[e] |
| $\mathbf{6}^{+\bullet}$-*sc*-oo | 3.73 | 1.445 | 47.52 | 19.15/26.72 |

[a] B2LYP/6-31G(d). [b] In/on ring with in-methoxy group. [c] In/on ring with out-methoxy group. [d] Carbonyl oxygen pointing in toward the adjacent pyridinium ring. [e] Carbonyl oxygen pointing out away from adjacent pyridinium ring.

(Figure 7). The anticlinal (*ac*) conformation had a $N_1C_2C_{2'}N_1$ dihedral angle of 136.2° at the B3LYP/6-31G(d) level and was 1.78 kcal/mol more stable than the synclinal (*sc*) conformation that was characterized by a considerably smaller $N_1C_2C_{2'}N_1$ dihederal angle of 59.4° (Table 1). The $C_2-C_{2'}$ distance in the *ac* conformation was nearly identical at all computational levels ($1.480 \pm 0.004$ Å) and slightly shorter than that observed for the *sc* conformation (1.489 Å; B3LYP/6-31G(d)). (See Supporting Information for more detailed structural parameters.) The greatest structural deviation as a function of computational level was observed for the $N_1C_2C_{2'}N_1$ dihedral angle, which decreased from 136.2° to 125.0° in the sequence B3LYP/6-31G(d) > MP2/6-31G(d) > MP2/6-31+G(d,p).

We suggest that the population of twisted *ac* and *sc* conformations in $\mathbf{7}^{2+}$ is a result of a compromise between electronic effects that prefer a planar structure to maximize delocalization and a steric effect that prefers a bisected conformation. In pyridinium ions $\mathbf{2}^{2+}-\mathbf{6}^{2+}$, the steric effect dominates and only a bisected, nearly perpendicular, conformation was located (Table 1). The steric effect could presumably be ameliorated by pyramidalization at nitrogen. However, the cost in lost aromatic resonance energy is clearly too much and the $(CH_3)N_1C_2C_{2'}$ and $(CH_3)N_{1'}C_{2'}C_2$ dihedral angles were less than 2° in all the dications. In the case of dications $\mathbf{5}^{2+}$ and $\mathbf{6}^{2+}$ a pool of bisected conformations exist as a result of rotational freedom around the $C_4-(OCH_3)$ and $C_4-(C{=}O)$ bonds, respectively. In $\mathbf{5}^{2+}$ the $C_4-O-CH_3$ angle is nearly 120° and the

**TABLE 3: Computed Structural Parameters for the Neutral Partner in the 2,2′-Bipyridinium Redox Process[a]**

| compound | isomer | $\Delta E_{rel}$ (kcal/mol) | $d(C_2-C_{2'})$ (Å) | $\angle N_1C_2C_{2'}N_{1'}$ (deg) | $\angle CH_3N_1C_2C_{2'}$ (deg) |
|---|---|---|---|---|---|
| **2** | *Z*-anti | 0 | 1.392 | 17.25 | 46.34/46.41 |
| | *E*-pp[a] | 2.63 | 1.392 | 158.72 | 66.92/16.63 |
| | *E*-anti | 3.24 | 1.375 | 179.99 | 64.12/64.23 |
| **3** | *Z*-anti | 0 | 1.384 | 8.58 | 53.67/51.64 |
| | *E*-anti | 2.93 | 1.375 | 180.00 | 66.03 |
| | *E*-syn | 3.34 | 1.382 | 160.82 | 52.78/55.55 |
| | *E*-pp | 4.65 | 1.393 | 161.30 | 69.06/14.12 |
| **4** | *Z*-anti | 0 | 1.390 | 15.87 | 47.35/47.40 |
| | *E*-pp | 2.13 | 1.391 | 159.77 | 14.94/67.12 |
| | *E*-anti | 2.64 | 1.374 | 179.99 | 63.59/63.72 |
| **5** | *Z*(ii)-anti | 0 | 1.380 | 7.54 | 53.25 |
| | *E*(ii)-anti | 2.00 | 1.372 | 180.00 | 65.70/65.69 |
| | *E*(ii)-pp | 2.68 | 1.384 | 161.98 | 68.06/20.99 |
| | *Z*(io)-anti | 2.85 | 1.381 | 9.07 | 53.16/51.27 |
| | *E*(ii)-syn | 3.52 | 1.378 | 161.53 | 55.22/55.24 |
| | *E*(io)-anti | 4.95 | 1.372 | 179.86 | 63.37/65.34 |
| | *E*(oi)-pp | 5.21 | 1.386 | 162.72 | 69.22/16.06 |
| | *E*(io)-pp | 5.71 | 1.385 | 161.79 | 66.73/20.70 |
| | *Z*(oo)-anti | 5.98 | 1.383 | 10.37 | 51.34/51.33 |
| | *E*(io)-syn | 6.56 | 1.379 | 161.10 | 53.35/54.78 |
| | *E*(oo)-anti | 7.78 | 1.373 | 180.00 | 63.05/62.98 |
| | *E*(oo)-pp | 8.14 | 1.387 | 162.70 | 67.96/15.4 |
| | *E*(oo)-syn | 9.49 | 1.381 | 159.74 | 51.49/51.56 |
| **6** | *Z*(ii)-anti | 0 | 1.415 | 25.01 | 40.78/40.99 |
| | *E*(ii)-syn | 1.59 | 1.414 | 151.20 | 28.84/28.66 |
| | *E*(ii)-pp | 1.82 | 1.414 | 153.71 | 12.91/59.81 |
| | *E*(ii)-anti | 5.65 | 1.390 | 180.00 | 62.49/62.46 |

[a] All data were collected at the B3LYP/6-31G(d) level. [b] pp = push−pull see text.

$C_4-O$ bond length is 1.309 ± 0.001 Å, indicative of substantial delocalization of electron density on oxygen into the pyridinium ring. As a result of the coplanar arrangement of the methoxy group and the pyridium ring, three conformations were located, one with both $O-CH_3$ bonds pointing "in" toward the adjacent pyridium ring (i−i), one with both $O-CH_3$ bonds pointing "out" away from the adjacent pyridium ring (o−o), and a third conformation with one "in" and one "out" methoxy group (i−o). The o−o conformation is the global minimum with the i-o 2.01 kcal/mol and the i−i conformation 4.09 kcal/mol higher in energy. The dihedral angles between the two pyridinium rings are very similar in the three conformations (91.6 ± 1.8°). The entire $-\mathbf{CO_2}CH_3$ group in $\mathbf{6}^{2+}$ is also coplanar with the pyridinium ring with the carbonyl oxygen pointing either "in" or "out". In $\mathbf{6}^{2+}$, however, the energies increase in the order i−i < i−o < o−o with substantially different inter-pyridinium ring dihedral angles of 109.8°, 103.7°, and 99.4°, respectively (see Supporting Information).

The sum of the angles around the dimethylamino group in $\mathbf{3}^{2+}$ is 360°, significantly larger than the 328.5° expected for a tetrahedral center. An $sp^2$-hybridized planar nitrogen is consistent with a large contribution of resonance form $\mathbf{3}^{2+}\mathbf{B}$ (Figure 3) and with the significant barrier measured (vide supra) for rotation around the $C_4-NMe_2$ bond.

**Radical Cation Redox Partners.** Bipyridinium radical cation $\mathbf{7}^{+\cdot}$ like its dication redox partner exists in two rotomeric minima on the B3LYP/6-31G(d) conformational surface. The anti-periplanar (*ap*) conformation adopts a $N_1C_2C_{2'}N_1$ dihedral angle of 165.57° and the 1.28 kcal/mol less stable synperiplanar (*sp*) conformation a $N_1C_2C_{2'}N_1$ dihedral angle of 16.75°.[21] For comparison, the two rings in the dication, $\mathbf{7}^{2+}$, are significantly less coplanar with $N_1C_2C_{2'}N_1$ angles of 136.19° in the *ac* conformer and 59.45° in the *sc* conformer. We attribute the greater degree of coplanarity in the radical cation to an electronic driving force to allow delocalization of the additional electron throughout the $\pi$-system. The decrease in the $C_2C_{2'}$ bond distance from 1.478 Å in the *ac* and 1.489 Å in the *sc* dication to 1.423 and 1.425 Å in the *ap* and *sp* radical cation, respectively, is also consistent with an increase in $\pi$-bond order and greater overlap between the two rings in the radical cation. The $HN_1C_2C_{2'}$ and $HN_{1'}C_{2'}C_2$ dihedral angles of 17.5° in the *sp* conformation reveal a subtle out-of-the-plane bend of the N−H bond. This can be attributed to a combination of a steric effect and electrostatic repulsion between the significant positive charges residing on the hydrogens. The greater distance between the N−H bonds in the *ap* conformation leads to a considerably smaller out-of-plane bend of 5.95°.

Radical cations $\mathbf{2}^{+\bullet}-\mathbf{6}^{+\bullet}$ also adopt two conformations but the methyl−methyl or methyl−hydrogen buttressing destabilize the periplanar structures and dictates formation of the anticlinal (*ac*) and synclinal (*sc*) rotomers (Table 2). The substituents on the pyridinium ring have little effect the $N_1C_2C_{2'}N_1$ dihedral angle which is remarkably similar in all *ac* (141.1° ± 2.8) and in all *sc* (44.4° ± 4) conformations. The *ac* rotomer is more stable than the *sc* rotomer in every case. The same out-of-plane bend of the substituent on the pyridinium nitrogen as observed in $\mathbf{7}^{+\bullet}$ was observed in these radical cations. The energetic loss of aromatic resonance energy as a result of this deformation is paid for by the increased delocalization afforded by the partial delocalization over both pyridinium rings that is allowed in the *ac* and *sc* conformations.

Remarkably, the sum of the angles around the dimethylamino group in $\mathbf{3}^{+\bullet}$ is 360° identical to that observed in $\mathbf{3}^{2+}$. However, the $C_4-N$ bond length, which is a better indicator of $\pi$-bond order, has increased from 1.337 Å in $\mathbf{3}^{2+}$ to 1.363 Å in *ac*-$\mathbf{3}^{+\bullet}$ and to 1.362 Å in *sc*-$\mathbf{3}^{+\bullet}$. For comparison, typical gas-phase C═N and C−N bond lengths found in nonstrained compounds are 1.21 and 1.46 Å, respectively.[22] This suggests that the $C_4-N$ $\pi$-bond order is approximately 0.49 in $\mathbf{3}^{2+}$ and 0.39 in $\mathbf{3}^{+\bullet}$.

**Neutral Redox Partners.** The two-electron reduction of $\mathbf{7}^{2+}$ leads to both *E* and *Z* isomers (Figure 8). The two heterocyclic rings in the $C_2$ symmetric **7Z** isomer are nearly coplanar. On

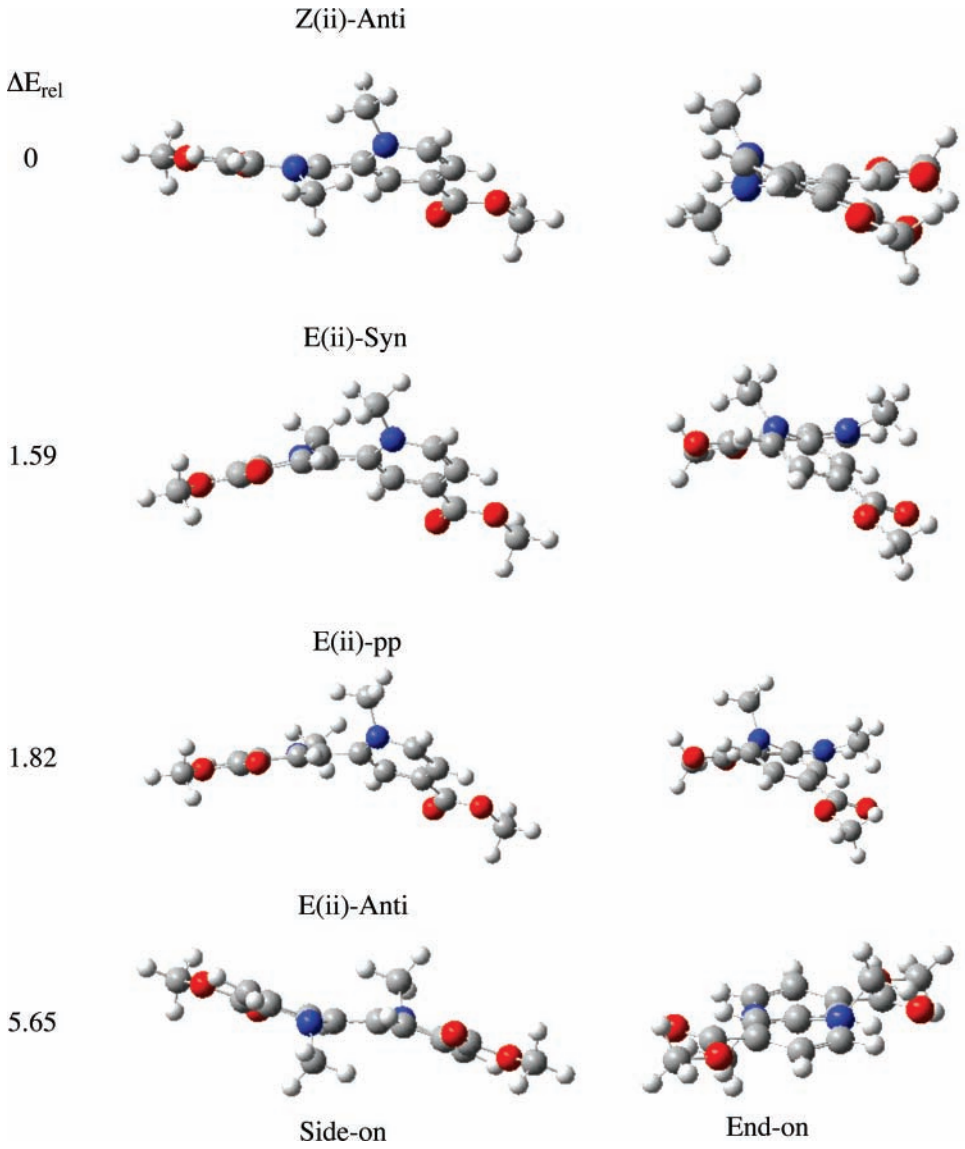


**Figure 9.** Side-on and end-on views of the isomers of **6**.

the other hand, the two heterocyclic rings are bent in the $C_i$ symmetric **7E** isomer. In both cases, however, $N_1C_2C_{2'}N_{1'}$ dihedral angles (**7Z**, 2.8°; **7E**, 180°) are as expected for a $\pi$-bond order of 2 between $C_2$ and $C_{2'}$ as implied by the resonance structure depicted in Figure 1. The presence of an olefinic linkage is further confirmed by the $C_2-C_{2'}$ bond distances of 1.377 and 1.373 Å in **7Z** and **7E**, respectively. Furthermore, the progressive decrease in this bond distance in $\mathbf{2}^{2+}$ > $\mathbf{2}^{+\bullet}$ > **7** is consistent with increasing inter-ring $\pi$-bond order in the series dication < radical cation < neutral. The increased pyramidalization at nitrogen in this same series is also consistent with decreasing aromatic character in the heterocyclic rings.

The most stable conformation of the *N*-methyl derivatives, **2**−**6**, by 2−3 kcal/mol, is the *Z*-(anti) isomer (Table 3). The destabilizing *N*-methyl/*N*-methyl interaction (Figure 1) in the *Z* isomers of **2**−**6** is relieved by both pyramidalization at nitrogen and twisting about the olefinic linkage. Both deformations are clearly visible in both side-on and end-on views of the *Z*-(anti) isomer of **6** in Figure 9. The *Z*-(syn) isomer was not found and does not appear to be a local minimum because of steric problems associated with placing the *N*-methyl groups on the same face (syn) of the pseudoplane defined by the olefinic linkage and the attached atoms. Twisting about the $C_2-C_{2'}$ olefinic linkage in the *Z*-(anti) isomer leads to $N_1C_2C_{2'}N_{1'}$ angles of 7.5° [*Z*(ii)-(anti)], 8.6°, 15.9°, 17.2°, and 25.0° in **5**, **3**, **4**, **2**, and **6**, respectively (Table 3). The twist angle is a rough function of the linear free energy substituent constant $\sigma_p$ (slope = 15.5; intercept = 15.4; $R^2$ = 0.8048) or $\sigma^+$ (slope = 9.0; intercept = 17.5; $R^2$ = 0.831), suggesting that the substituent at $C_4$ plays an important role in stabilizing the twisted olefinic linkage.[23]

The $A_{1,3}$ strain (Figure 1) in the *E* isomers of **2**−**6** is also ameliorated by both pyramidalization at nitrogen and twisting about the olefinic linkage. In the *E* conformations of **3**, **5**, and **6**, however, the syn isomer was located reflecting the absence of the steric interaction which prevents its population in the *Z* isomer. In the *E*-syn conformations of **3** and **5**, the average $\mathbf{CH_3N_1C_2C_{2'}}$ dihedral angle is 53.7 ± 2.3° and the average sum of angles around the nitrogen is 350.8 ± 1.2°, both reflecting a significant degree of pyramidilization. In contrast, in the *E*(in−in)-syn conformation of **6** the average $\mathbf{CH_3N_1C_2C_{2'}}$/$\mathbf{CH_3N_{1'}C_{2'}C_2}$ angle is only 28.75 ± 0.09° and the average sum of the angles around the two ring nitrogens is 358.8 ± 0.1°. In addition, the $C_2C_{2'}$ bond length of 1.414 Å is substantially longer and the $N_1C_2C_{2'}N_{1'}$ torsional angle of 151.2° is considerably greater than

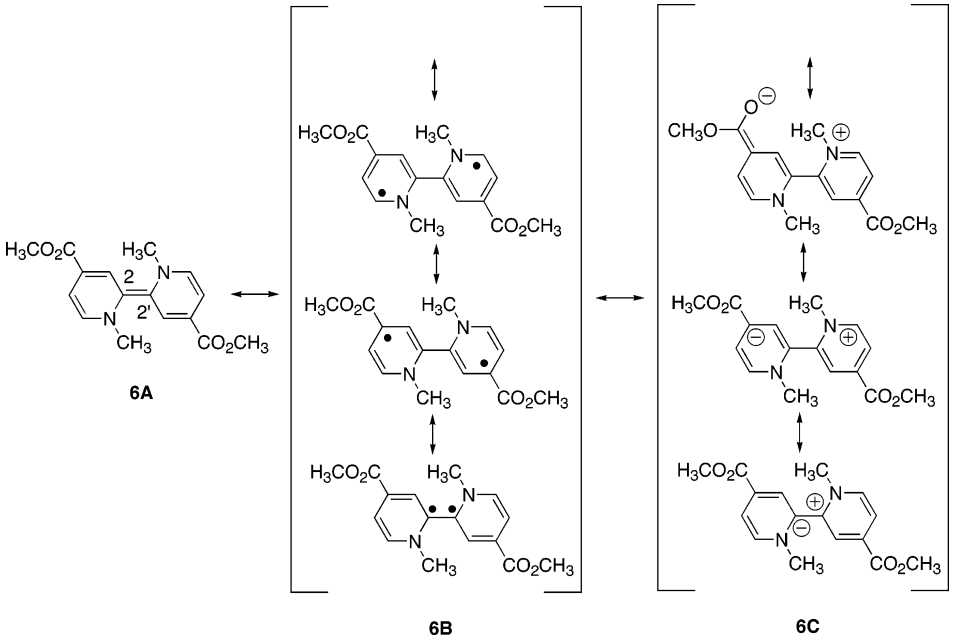


in the syn conformers of **3** and **5** (Table 3). We suggest that this structural deformation reflects a decrease in the $C_2-C_{2'}$ bond order and can be explained by a significant contribution of the captodatively[24] stabilized resonance forms **6B** and/or the zwitterionic resonance forms **6C**.

A third, very interesting, structure that we refer to as the push−pull (pp) conformer was also located on the *E* conformational energy surface. In this conformation the two ring nitrogens are pyramidalized to very different extents (Figure 9 and Table 3). For example, in **6** *E*(in−in)-pp (Table 3) the two $CH_3N_1C_2C_{2'}$ angles are 12.9° and 59.8°. We suggest that the population of the pp conformation reflects the contributions of zwitterionic resonance forms **6C** and in particular the topmost **6C** resonance form that can clearly rationalize the tendency toward planarization of one of the two heterocyclic rings. To explore this in more detail, we computationally examined the conformational surface for the *E* and *Z* isomers of the neutral redox partner of 1,1′-dimethyl-4-(i)-(carbomethoxy)-4′-(o)-methoxy-2,2′-bipyridinium, **13**. (See Supporting Information for structural details.) In **13** only the *E*-pp conformation with the methoxy group on the ring with the most planar nitrogen was located. All attempts to start with a conformation that placed the methoxy group on the ring bearing the more pyramidalized nitrogen resulted in minimization to form the more stable *E*-pp conformation with the methoxy on the more planar ring. This is consistent with the importance of resonance form **13A** in which the methoxy group can *push* electron density into the ring with pyridinium ion character and the carbomethoxy group can *pull* the electron density out of the less planar negatively charged heterocyclic ring. In the *Z* isomers of **2**−**6**, adopting the anti conformations minimizes the destabilizing *N*-methyl/*N*-methyl interactions. In **13-Z(i−o)** increased *N*-methyl/*N*-methyl interaction is tolerated to enjoy the electronic advantage of the push−pull conformation. All attempts to locate the anti conformation of **13-Z(i−o)** failed and only **13-Z(i−o)pp** characterized by two different $\mathbf{C}H_3\mathbf{N}C_2\mathbf{C}_{2'}$ angles (56.20° and 31.86°) was located. However, the $\mathbf{C}H_3\mathbf{N}C_2\mathbf{C}_{2'}$ angle of 31.86° in **13-Z(i−o)pp** is larger than that observed in the *Z*-pp conformations of **2**−**6** (Table 3; 16.4 ± 4.5°) and is indicative of an *N*-methyl/*N*-methyl steric interaction that prevents complete flattening of the methoxy bearing heterocyclic ring.

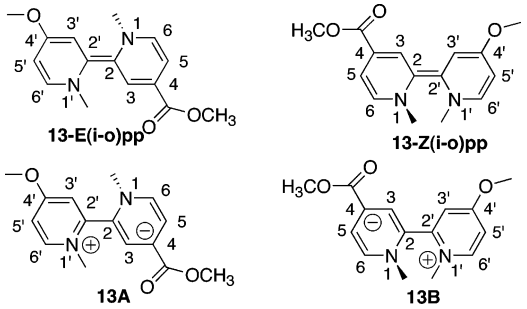


## Conclusion

In this study we have examined the effect of 4,4′ substituents (H, $NMe_2$, Cl, OMe, and $CO_2Me$) on the electrochemical behavior of 2,2′-bipyridinium ions. In addition, we reported the first successful attempt to collect a complete set of UV−vis spectra for a 2,2′-bipyridinium ion and its one- and two-electron-reduced products.[25] A detailed computational study has revealed remarkable substituent effects on the energies and on the conformational energy surface of all three members of these one- and two-electron redox couples. This information will be of value to workers who wish to incorporate these species into devices or supramolecular structures.

## Experimental Section

**2,2′-Bipyridine *N*,*N*′-Dioxide, 8**.[8] A 15 mL solution of 30% hydrogen peroxide was added to 2,2′-bipyridine (38.5 mmol, 6.0 g) in 40 mL of glacial acetic acid at a rate that maintained the temperature between 70 and 80 °C. This mixture was stirred at 75 °C for an additional 8 h. The colorless solution was then cooled to room temperature, and a copious amount (500 mL) of acetone was added to precipitate the product as a white solid, which was collected by filtration and air-dried. The white solid was then recrystallized from hot water to give 6.4 g (36.7 mmol, 94% yield) of the product. $^1$H NMR (400 MHz; $D_2O$; ppm): $\delta$ 7.76 (4H, m), 7.85 (2H, m), 8.47 (2H, m).

**4,4′-Dinitro-2,2′-bipyridine *N,N′*-Dioxide, 9**.[9] A solution of 2,2′-bipyridine *N,N′*-dioxide, **8**, (23.9 mmol, 4.5 g) in 13 mL of oleum−sulfuric acid was cooled to 0 °C. Fuming nitric acid (10 mL) was carefully added, and the mixture was stirred at 100 °C for 8 h. The solution was then cooled to 0 °C and very cautiously poured on ice−water (100 g). The yellow product was filtered off and washed with water until neutral (**9**; yellow powder yield 4.5 g, 10.8 mmol). $^1$H NMR (400 MHz; DMSO-$d_6$; ppm): $\delta$ 8.37 (dd, $J = 3.3$, 7.3 Hz, 2H), 8.60 (d, $J = 7.2$ Hz, 2H), 8.69 (d, $J = 3.3$ Hz, 2H).

**4,4′-Dichloro-2,2′-bipyridine *N,N′*-Dioxide, 10**.[8] A suspension of 4,4′-dinitro-2,2′-bipyridine *N,N′*-dioxide (13.6 mmol, 3.8 g) in glacial acetic acid (60 mL) and acetyl chloride (40 mL) was stirred for 4 h at 100 °C. The resulting yellow-brown solution was cooled to 0 °C and poured on ice (125 g) and neutralized with a concentrated sodium hydroxide solution. An off-white solid was filtered off, washed with water, and air-dried (**10** 80% yield 2.8 g 10.5 mmol).

**4,4′-(Dimethylamino)-2,2′-bipyridine *N,N′*-Dioxide, 11, and 4,4′-(Dimethylamino)-2,2′-bipyridine, 12**.[10] A suspension of 996 mg of 4,4′-dichloro-2,2′-bipyridine *N,N′*-dioxide (3.89 mmol) in 150 mL of DMF was refluxed under nitrogen for 48 h. The solvent was evaporated nearly completely, and the crude **11** (brown paste) was dissolved in 100 mL of chloroform. Phosphorus trichloride (8.5 mL, 97 mmol) was added dropwise to the cooled solution at 0 °C. The reaction was then refluxed for 3 h and then poured onto 250 mL of ice water. The chloroform layer was washed with 3 × 50 mL of water and the combined aqueous fractions were concentrated under vacuum to 80 mL and made alkaline with saturated aqueous sodium hydroxide. The resulting precipitate was recrystallized twice from water/methanol (1.5 v/v) to give 180 mg of the beige product **12** (0.88 mmol, 19%; mp. 234−235 °C). $^1$H NMR (DMSO-$d_6$): $\delta$ 3.03 (s, 12H), 6.65 (dd, $J = 2.6$, 5.9 Hz, 2H), 7.68 (d, $J = 2.6$ Hz, 2H), 8.21 (d, $J = 5.9$ Hz, 2H).

**1, 1′-Dimethyl-4,4′-(dimethylamino)-2,2′-bipyridinium Tetrafluoroborate, $3^{2+}$**. A mixture of 4,4′-(dimethylamino)-2,2′-bipyridine (0.001 mol) and trimethyloxonium tetrafluoroborate (0.002 mol) in 30 mL of dichloromethane was stirred at room temperature for 48 h. The solvent was evacuated in vacuo and the product recrystallized three times from $CH_3CN$ and diethyl ether to give the beige product, $\mathbf{3}^{2+}$ (0.33 g; 0.75 mmol; 75% yield), mp > 240 °C. $^1$H NMR (400 MHz; $CD_3CN$; ppm): $\delta$ 3.19 (s, 6H), 3.25 (s, 6H), 3.60 (s, 6H), 6.9−7.02 (m, 4H), 8.04 (d, $J = 7.5$ Hz, 2H). $^1$H NMR (400 MHz; $D_2O$; ppm): $\delta$ 3.19 (s, 6H), 3.25 (s, 6H), 3.66 (s, 6H), 7.00 (dd, $J = 7.7$, 3.1 Hz, 2H), 7.07 (d, $J = 3.1$ Hz, 2H), 8.11 (d, $J = 7.7$ Hz, 2H). $^{13}$C NMR (100 MHz; $CD_3CN$; ppm): $\delta$ 41.1 (q, $J = 136$ Hz), 41.2 (q, $J = 136$ Hz), 43.8 (q, $J = 145$ Hz), 109.5 (d, $J = 172$ Hz), 112.1 (d, $J = 172$ Hz), 144.1 (s), 145.8 (d, $J = 188$ Hz), 157.6 (s). Anal. Calcd For $C_{16}H_{24}N_4B_2F_8$: C, 43.09; H, 5.42; N, 12.56. Found: C, 42.88; H, 5.28; N, 12.35.

**Optical Spectra (Figure 6).** The optical spectra of the three members of the **6** redox series (Figure 6) were measured in glass cells equipped with an ESR tube and a quartz optical cell. Dry acetonitrile was distilled into the cell, the cell was degassed, and the apparatus was sealed under vacuum. Reduction of the $\mathbf{6}^{2+}$ solution was achieved by stepwise contact with 0.2% Na−Hg amalgam.

**Acknowledgment.** We thank the Professor Frank Jensen (Odense University, Denmark) for valuable comments and the National Science Foundation (U.S.A.) and Fundação Para a Ciência e Tecnologia through its Centro de Química Estrutural (J.P.T.) for their generous support of this research.

**Supporting Information Available:** Tables of energies and structural data. Figures giving a Hammett plot, NMR spectra, and a UV−vis spectrum. This material is available free of charge via the Internet at http://pubs.acs.org.

## References and Notes

(1) Weidel, H.; Russo, M. *Monatshefte* **1882**, *3*, 850−885.
(2) Michaelis, L. *Biochem. Z.* **1932**, *250*, 564−567.
(3) Summers, L. A. *The Bipyridinium Herbicides*; Academic Press: New York, 1980.
(4) Monk, P. M. S. *The Viologens. Physicochemical Properties, Synthesis and Applications of the Salts of 4,4′-Bipyridine*; John Wiley & Sons: Chichester, England 1998; p 311.
(5) (a) Pepitone, M. F.; Jernigan, G. G.; Melinger, J. S.; Kim, O.-K. *Org. Lett.* **2007**, *9*, 801−804. (b) Kim, Y.; Das, A.; Zhang, H.; Dutta, P. K. *J. Phys. Chem. B* **2005**, *109*, 6929−6932.
(6) Clennan, E. L. *Coord. Chem. Rev.* **2004**, *248*, 477−492.
(7) Zhang, D.; Dufek, E. J.; Clennan, E. L. *J. Org. Chem.* **2006**, *71*, 315−319.
(8) Anderson, S.; Constable, E. C.; Seddon, K. R.; Turp, J. E.; Baggott, J. E.; Pilling, M. J. *J. Chem. Soc., Dalton Trans.* **1985**, 2247−2261.
(9) Kavanagh, P.; Leech, D. *Tetrahedron Lett.* **2004**, *45*, 121−123.
(10) Wehman, P.; Dol, G. C.; Moorman, E. R.; Kamer, P. C. J.; van Leeuwen, P. W. N. M. *Organometallics* **1994**, *13*, 4856−4869.
(11) Negele, S.; Wieser, K.; Severin, T. *J. Org. Chem.* **1998**, *63*, 1138−1143.
(12) Reich, H. J. *WinDNMR: Dynamic NMR Spectra for Windows*; *Journal of Chemical Education* Software 3D2, 1996.
(13) Kalatzis, E.; Kiriazis, L. *J. Chem. Soc., Perkin Trans. 2* **1989**, 179−185.
(14) Petersilka, M.; Grossmann, U. J.; Gross, E. K. U. *Phys. Rev. Lett.* **1996**, *76*, 1212−1215.
(15) Dreuw, A.; Head-Gordon, M. *J. Am. Chem. Soc.* **2004**, *126*, 4007−4016.
(16) Frisch, M. J.; Trucks, G. W.; Schlegel, H. B.; Scuseria, G. E.; Robb, M. A.; Cheseman, J. R.; Montgomery, J. A, Jr.; Vreven, T.; Kudin, K. N.; Burant, J. C.; Millam, J. M.; Iyengar, S. S.; Tomasi, J.; Barone, V.; Mennucci, B.; Cossi, M.; Scalmani, G.; Rega, N.; Petersson, G. A.; Nakatsuji, H.; Hada, M.; Ehara, M.; Toyota, K.; Fukuda, R.; Hasegawa, J.; Ishida, M.; Nakajima, T.; Honda, Y.; Kitao, O.; Nakai, H.; Klene, M.; Li, X.; Knox, E.; Hratchian, H. P.; Cross, J. B.; Adamo, C.; Jaramillo, J.; Gomperts, R.; Stratmann, R. E.; Yazyev, O.; Austin, A. J; Cammi, R.; Pomelli, C.; Ochterski, J. W.; Ayala, P. Y.; Morokuma, K.; Voth, G. A.; Salvador, P.; Dannenberg, J. J.; Zakrzewski, V. G.; Dapprich, S.; Daniels, A. D.; Strain, M. C.; Farkas, O.; Malick, D. K.; Rabuck, D.; Raghavachari, K.; Foresman, J. B.; Ortiz, J. V.; Cui, Q.; Baboul, A. G.; Clifford, S.; Cioslowski, J.; Stefanov, B. B.; Liu, G.; Liashenko, A.; Piskorz, P.; Komaromi, I.; Martin, R. L.; Fox, D. J.; Keith, T.; Al-Laham, M. A.; Peng, C. Y.; Nanayakkara, A.; Challacombe, M.; Gill, P. M. W.; Johnson, B.; Chen, W.; Wong, M. W.; Gonzalez, C.; Pople, J. A. *Gaussian 03*, revision A.1; Gaussian, Inc.: Pittsburgh, PA, 2003.
(17) Becke, A. D. *J. Chem. Phys.* **1993**, *98*, 5648−5652.
(18) Stephens, P. J.; Devlin, F. J.; Chabalowski, C. F.; Frisch, M. J. *J. Phys. Chem.* **1994**, *98*, 11623−11627.
(19) Hofmann, H.-J.; Cimiraglia, R.; Tomasi, J. *J. Mol. Struct. (THEOCHEM)* **1986**, *139*, 213−219.
(20) Cramer, C. J. *Essentials of Computational Chemistry. Theories and Models*; John Wiley & Sons Ltd.: Chichester, England, 2002.
(21) RHF calculations using the standard STO-3G basis set were used to partially optimize the ap conformation of $\mathbf{7}^{+\bullet}$ The $C_2-C_{2'}$ distance (1.449Å) and the $N_1C_2C_{2'}N_{1'}$ dihedral angle (170.1°) were in reasonable agreement with our calculated B3LYP/6-31G(d) value of 1.423 Å and 165.57°, respectively. Hofmann, H.-J.; Cimiraglia, R.; Tomasi, J. *J. Chem. Res. S* **1987**, 48−49.
(22) Lide, D. R. *CRC Handbook of Chemistry and Physics*, 86th ed.; Taylor & Francis: Boca Raton, FL, 2005−2006.
(23) Only a poor correlation was observed with a variety of radical substituent constants. Multiparameter fits were not pursued. Dust, J. M.; Arnold, D. R. *J. Am. Chem. Soc.* **1983**, *105*, 1221−1227.
(24) Fossey, J.; Lefort, D.; Sorba, J. *Free Radicals in Organic Chemistry*; John Wiley & Sons: New York, 1995; p 307.
(25) Optical spectra for all three redox partners in 4,4′-bipyridinium ions have been reported. Porter, W. W., III; Vaid, T. P. *J. Org. Chem.* **2005**, *70*, 5028−5035.